MODELING CONVENTIONAL TWO-DIMENSIONAL DRYING OF RADIATA PINE BASED ON TRANSVERSAL EFFECTIVE DIFFUSION COEFFICIENT

Y.A. GATICA[†], C. H. SALINAS[‡] and R.A. ANANIAS[§]

[†] *Doctoral student, Department of Wood Engineering, U. del Bío-Bío, Collao 1202, Concepción, CHILE. ygatica@ubiobio.cl*
[‡] *Department of Mechanical Engineering, U. del Bío-Bío, Collao 1202, Concepción CHILE. casali@ubiobio.cl*
[§] *Department of Wood Engineering, U. del Bío-Bío, Collao 1202, Concepción, CHILE. ananias@ubiobio.cl*

***Abstract*— We modeled conventional two-dimensional drying of radiata pine (*Pinus radiata*) wood using the concept of effective diffusion extended to overall drying process. Effective diffusion coefficients were determined experimentally on the transversal plane and depended exponentially on the moisture content. These coefficients were characterized by two parameters determined through optimization within the context of an inverse problem. Spatially variable convection coefficients were determined in the same manner. Experiments using constant drying 44/36 (ºC/ºC) were carried out in order to determine transitory spatial distributions of moisture and drying curves, which were then used to determine and validate the model parameters. The mathematical model consisted of a partial, nonlineal, differential equation of the second order, was characterized by coefficients that varied exponentially with moisture content, integrated numerically through the finite volume method. Results of two-dimensional simulations for isothermal drying of radiata pine timber, correlated with experimental data, are shown: a) Transitory distribution of moisture gradients, b) drying curves and c) parameter of mathematical model (effective diffusion and mass convection coefficients)**.

***Keywords*—drying, wood, radiata pine, diffusion**

I. INTRODUCTION

Wood is a particularly non-homogeneous biomaterial with a porous anisotropic structure. For purposes of flow transport, wood is often described in terms of its properties (diffusiveness, permeability, porosity, etc.). It is taken to be a continuous, homogeneous material. However, the properties of wood differ markedly according to the spatial direction (radial, tangential, longitudinal) in which it is observed: known orthotropic behavior of wood (Siau, 1984). Moreover, there is a preferential drying direction for moisture transport, normally towards the surface exposed to the drying environment and, therefore, relied on one-dimensional modeling. Nevertheless, depending on how the wood is placed in the dryer, could result in one or more preferential directions, like discussed in Pang (1996) for relevant two-dimensional transversal transport in drying processes.

Modeling the moisture transport within wood can be done with classic diffusive models such as those suggested by Stamm (1964) or Siau (1984); those based on the thermodynamics of irreversible processes, as established by Luikov (1966); and those developed from Whitaker's multiphase approach (Whitaker, 1977).

In one dimensional models: Plumb *et al*. (1985) and Nasrallah and Perré (1988) have used the Whitaker focus. Furthermore, Jen and Chen (1991) applied a more analytical methodology following the Luikov formulation. In two-dimensional drying modeling: Cloutier and Fortin (1991, 1993) and Perré *et al*. (1993) used the moisture potential concept of Luikov's approach, whereas Turner (1996) used a model in accordance with Whitaker's proposition and incorporated aspects associated with deformation during drying. Works of three-dimensional drying simulations of wood had been performed according to Withaker`s jobs by Perré and Turner (1999) and using the approximation of Luikov by Younsi *et al.* (2006).

The properties characterizing the transport of moisture have been determined (Siau, 1995; Tremblay *et al*., 2000; Nabhani *et al*., 2003).

This study deals with diffusive models, traditionally used for simulating the drying of conifer and broadleaf wood below the fiber saturation point (FSP). Diffusive transport is the dominant mechanism in this drying range (Smith and Langrish, 2008; Hukka, 1999; Pang, 1997), but above the FSP, diffusive models are hindered by other dominant transport phenomena such as capillarity and permeability (Keey *et al*., 2000). By the way, the researchers have formulated models that made difference above and below FSP like the one proposed by Davis *et al*. (2002). Nonetheless, diffusive models can be used beyond the hygroscopic range by obtaining an effective diffusion coefficient (EDC) for water as generally done for porous materials (Simpson and Liu, 1997; Hukka, 1999; Chen, 2007), and applying it to the simulation of drying kinetics over the entire moisture range of conifer woods (Rozas *et al*., 2009). Other studies have explored the determination of diffusive coefficients using two experimental methods solved through the finite difference method (Droin *et al*., 1988) or applied to the case of one-dimensional transport in radiata pine (Gatica *et al*., 2011), the approach taken by the present authors.

In numerical terms, the finite volume method (Patankar, 1980) was implemented in order to integrate the two-dimensional diffusive transport equation. A central difference was used for the second-order derivatives and an implicit Euler scheme for the advances in time.

The parameters that ultimately determined the relationship between moisture content and moisture flow were calculated by solving the following inverse problem: Given a known drying curve and known moisture distributions, we determined the EDCs that resulted in the lowest differences between the experimental and simulated moisture distributions. Moreover, due to the marked differences in convection levels at the wood/drying interface (Davis and Moore, 1982), we established an adequate distribution of the mass convection coefficient value at this interface. Other authors have also sought out diffusive and convective coefficients by solving an inverse problem, like presented by Jen and Chen (1991) who resolved an inverse mass transport problem using the finite difference method.

The objective of this work is to model the two-dimensional drying of radiata pine considering the entire moisture range (under and above the FSP) and using the extended concept of EDC, proposed by Comstock (1963). The EDC was used for two-dimensional modeling on the transversal plane of *Pinus radiata* (D. Don) wood. Previous experiments allowed us to use transitory distributions of moisture content gradients and drying curves, which are useful for determining properties and validating the proposed model.

II. MATERIALS AND METHODS

A. Description of the experiments

Radiata pine wood was dried in a climate-controlled chamber for convective drying at a low temperature: Average transversal air flow of 1.6 m/s and dry and wet bulb temperatures of 44 and 36 °C, respectively. For the experiment, seven wood blocks (P1 to P7; 40x40x300 mm) were cut transversally (radial and tangential plane). The samples were selected of a twenty-year old radiata pine, tree growing in the Bio-Bio region in the south of Chile, according to Chilean norms for testing and procedure to determine moisture content (INN, 1984 and 1986). To favor a two-dimensional flow, the transversal cuts at each end of the blocks were sealed with silicon and aluminum foil.

We performed two experiments (see Fig. 1). In the first, four blocks of wood (P1 to P4) were subjected to the drying process. Block P1 was connected to a scale (A&D model DF4000 with accuracy 0.1 g and measure error± 0.1 g) and its variations in weight were measured continuously. This block was dried for 24 hours in a Memmert Oven conditioned with dry air at 103 ºC to determine its dry (anhydrous) mass, which was then used to calculate the water mass (M) according to Eq. (1). Block P3 was also used for discreet records of transitory moisture values, providing a counter-sample for the continuous evaluation.

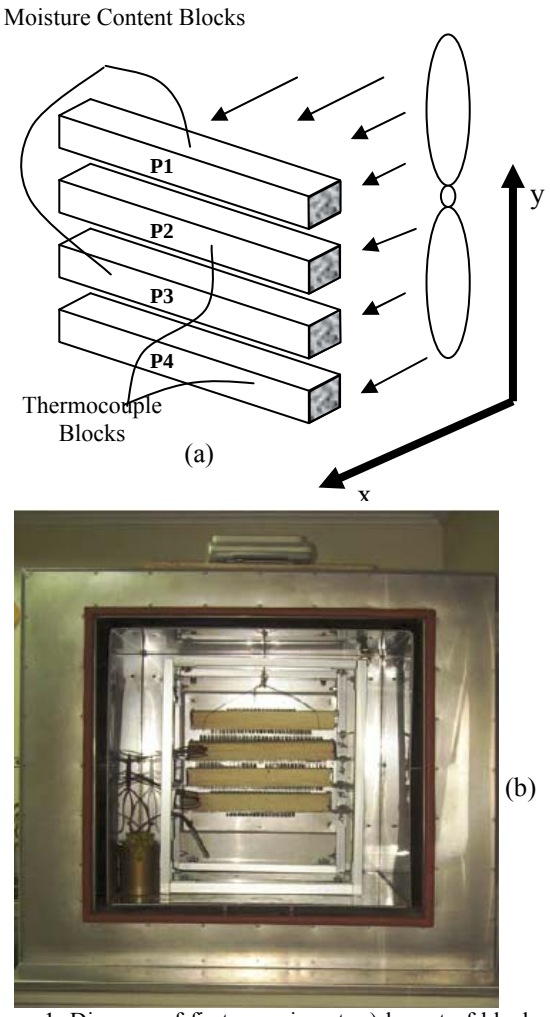

Figure 1. Diagram of first experiment: a) layout of blocks, b) view of the set-up inside the climate chamber.

We used these data to obtain an experimental drying curve and to select the drying times at which spatial moisture distributions would be determined (four drying times were selected). Blocks P2 and P4 were used to monitor the temperatures inside the wood using T-type thermocouples and an acquisition system (Fluke, Hydra II model, accuracy ± 0.5 ºC). Both the A&D scale and the Hydra II were connected to a computer, where the respective data were stored (see Fig. 2).

$$MC = \left(\frac{m_m - m_d}{m_d} \right) * 100 \quad ; \quad M = \frac{MC * m_d}{100} \qquad (1)$$

where MC (%) is the moisture content, m_m (kg) is the wet mass, m_d (kg) is the anhydrous mass, and M (kg) is the water mass.

The second experiment consisted of subjecting the three remaining blocks (P5 to P7) to the same drying conditions. Block P5 was used to measure the average water mass and was monitored constantly on a scale, whereas blocks P6 and P7 were used to take transitory samples of two-dimensional moisture content distributions at the four times determined in the earlier experiment. For this, blocks P6 and P7 were removed at the times indicated and cut transversally (destructive sample

Figure 2. Boeco balance used to determine the mass of each section obtained from blocks P6 and P7.

evaluation) to one quarter their length (75 mm). The sides exposed by the cut were sealed, what remained of the blocks was returned to the chamber, and the drying process continued. The sample obtained was subdivided into 25 equal parts along its transversal cut. The moisture content of each of these was determined based on its dry and wet weights using a Boeco balance (model BPB32, Accuracy 1 mg with measure error ± 0.05 %), shown in the Fig. 2.

This process was repeated for the three remaining quarters of block P6 at the previously selected drying times. Block P7 acted as a counter-sample for block P6.

B. Coefficient determination

After an exploratory study with two types function to describe distributions of EDC inside of wood during drying process: potential and exponential type function suggested by Pang (1996) and Hukka (1999), respectively, the latter was selected because it presented better results. When it is applied to the case of isothermal drying, this coefficient can be described by the following expression:

$$D(M) = \exp\left(\alpha + \beta * \tilde{M}\right) \qquad (2)$$

where $\tilde{M} = \min\left(\frac{m_m}{m_d}, FSP\right)$

$FSP = 0.603 - 0.001 * T_d$ (Bramhall, 1979)

T_d dry bulb temperature (K)

This required the determination of two parameters: α and β.

The mass convection coefficient S (m^2/s) is a function of the type and form of the interface and the properties of the wood and the drying environment. However, constant values that represent a spatial and temporal measurement of this coefficient are commonly assumed. Consequently, the two-dimensional phenomenon is best represented by four convective coefficient distributions, S_w, S_e, S_s, and S_n, one for each characteristic surface, as shown in Fig. 3. This kind of distribution was performed after exploratory evaluation and according with the reported in the literature by Davis and Moore (1982) or more recently by Yang and Fu (2001).

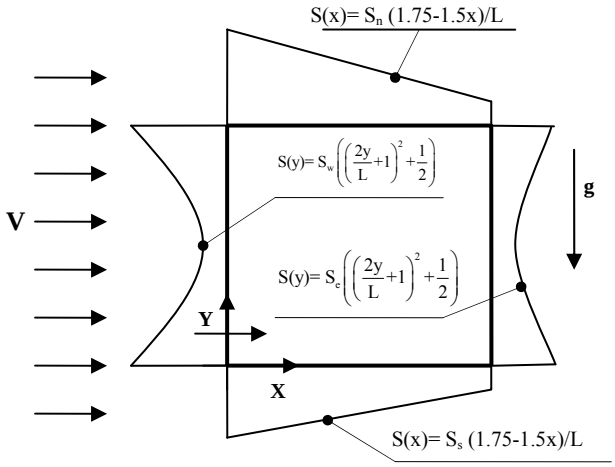

Figure 3. Scheme of transversal section where cross flow is represent by arrow and symbol **V**, the boundary of wood by thick line and the distribution of mass convection coefficient (S) with thin line.

We determined parameters α and β, which define the EDC in function of M, and the mass convection coefficients S (S_w, S_e, S_s, and S_n) by solving the following inverse problem: Given a known spatial moisture distribution at certain points along the drying curve, we calculated the parameters α, β, and S in order to obtain a minimal difference between the experimental and simulated moisture distributions.

We performed an extensive search for these parameters, selecting those that presented a minimum difference between the experimental and simulated data (see Fig. 4). This difference was determined from the following error function:

$$\text{Error} = \frac{1}{n}\sum_{i=1}^{n} \text{abs}\left(\frac{M_{Sim} - M_{Exp}}{M_{Exp}}\right) \qquad (3)$$

```
procedure Determine α, β and S
    Initial Guess
    Mesh Generation
    min < α < max
    min < β < max
    min < S < max
    for S ← Smin to Smax do
        for S ← βmin to βmax do
            for α ← αmin to αmax do
                Simulate with α, β and S
                Calculate error
                if error < errormin
                    errormin = error
                    Sopt = S
                    αopt = α
                    βopt = β
                end if
            end for
        end for
    end for
    α = α opt
    β = βopt
    S = Sopt
    Simulate Diffusion Equation
end procedure
```

Figure 4. Search pseudocode: α, β and S.

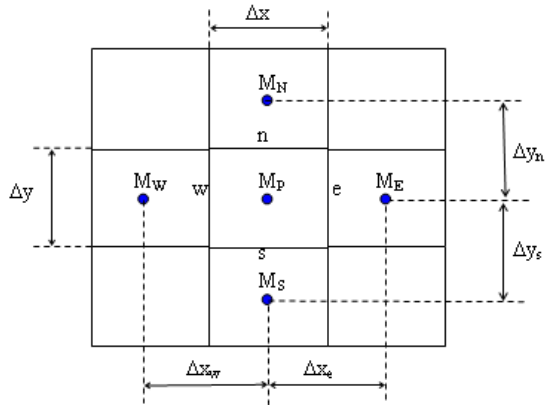

Figure 5. Discretization scheme.

III. MATHEMATICAL/NUMERICAL MODEL

The mathematical model consists of a partial, differential, non-linear, second-order equation that describes the two-dimensional transitory diffusion of a water mass M (kg_w).

$$\frac{\partial M}{\partial t}=\frac{\partial}{\partial x}\left(D(M)\frac{\partial M}{\partial x}\right)+\frac{\partial}{\partial y}\left(D(M)\frac{\partial M}{\partial y}\right) \quad (4)$$

where D(M) is the EDC (m^2/s), a function of water mass M.

The initial conditions for a domain of V with a contour of Ω are as follows:

$$\begin{aligned} &M(t=0)=M_0 \ \text{ in } \ V \ \text{ (Initial)} \\ &D\frac{\partial M}{\partial \mathbf{n}}=S(M_\infty-M_s) \ \text{ in } \ \Omega \ \text{ (convection)} \end{aligned} \quad (5)$$

The numerical integration of this differential model was done using the finite volume method. For this, we considered the domain 0<(x,y)<L subdivided into **N**=ni*nj finite volumes V_{ij} (i=1, ni; j=1,nj), representing the average value of the variable (M_P) in the centroid and the values of M in the adjacent volumes: behind (M_W), forward (M_E), below (M_S), and above (M_N). The limits of the finite volume (FV) centered on P were identified by w, e, s, and n, respectively (see Fig. 5).

By integrating Eq. (4) according to generic FV shown in the Fig. 5, evaluating the integrals of the transient term according to the mid-point rule and considering fundamental theorem of calculus, we have:

$$\begin{aligned} \frac{\partial M}{\partial t}dxdy=&\left[\left(D\frac{\partial M}{\partial x}\right)_e-\left(D\frac{\partial M}{\partial x}\right)_w\right]\Delta y+ \\ &\left[\left(D\frac{\partial M}{\partial y}\right)_n-\left(D\frac{\partial M}{\partial y}\right)_s\right]\Delta x \end{aligned} \quad (6)$$

The derivatives of M in the central form and the temporal derivative in the delayed form define an implicit Euler diagram:

$$\begin{aligned} &\frac{M_P-M_P^0}{\Delta t}\Delta x\Delta y= \\ &\left(D_e\frac{M_E-M_P}{\Delta x_e}\right)\Delta y-\left(D_w\frac{M_P-M_W}{\Delta x_w}\right)\Delta y+ \\ &\left(D_n\frac{M_N-M_P}{\Delta y_n}\right)\Delta x-\left(D_s\frac{M_P-M_S}{\Delta y_s}\right)\Delta x \end{aligned} \quad (7)$$

where M^0 represents the value of M in the previous period (known).

Now by grouping terms, we can write the generic algebraic equation for an FV centered on the P node:

$$a_PM_P+a_EM_E+a_wM_W+a_NM_N+a_SM_S=b_P \quad (8)$$

where

$$\begin{aligned} &a_t=\frac{\Delta x\Delta y}{\Delta t}; \quad a_E=-\frac{D_e\Delta y}{\Delta x_e}; \quad a_W=-\frac{D_w\Delta y}{\Delta x_w}; \\ &a_N=-\frac{D_n\Delta x}{\Delta y_n}; \quad a_S=-\frac{D_s\Delta x}{\Delta y_s} \\ &a_P=a_t-\left(a_W+a_E+a_N+a_S\right) \\ &b_P=a_tM_P^0 \end{aligned}$$

Thus, we can write **N**-2 (ni+nj-2) equations of type (8) (one for each internal volume). Two (ni+nj-2) were eliminated because the volumes of the ends are special (not generic), since they must incorporate the contour conditions of convection. In particular, for a contour that coincides with e in x=L, the convection condition described by Eq. (5), defines a mass flow (q_m) of:

$$q_m=\left(D\frac{\partial M}{\partial x}\right)_e=S\left(M_\infty-M_e\right) \quad (9)$$

The value of the variable at end e (M_e) is determined by linear extrapolation based on the values of M in P and W. That is:

$$M_e=M_P\left(1+\frac{\Delta x_e}{2\Delta x_w}\right)-\frac{\Delta x_e}{2\Delta x_w}M_W \quad (10)$$

By incorporating these definitions in Eq. (6) and grouping the terms to take them to the form of Eq. (8):

$$\begin{aligned} &a_E=0 \\ &a_W=-\left(\frac{S\Delta x_e\Delta y}{2\Delta x_w}+\frac{D_w\Delta y}{\Delta x_w}\right) \\ &a_P=a_t-\left(a_E+a_W+a_N+a_S\right)+S\Delta y\left(1+\frac{\Delta x_e}{2\Delta x_w}\right) \\ &b_P=a_tM_P^0+SM_\infty\Delta y \end{aligned}$$

a_N ; a_S ; a_t as defined in the generic equation

Expressions for contours located at x=0, y=0, and y=L can be obtained similarly.

Thus, we obtained a dominant penta-diagonal algebraic equation system of **N**x**N**, which is solved repetitively through the Gauss Saidel method (Lapidus and Pinder, 1982). The solutions report spatial moisture distributions.

IV. RESULTS

Radiata pine wood showed a classical experimental drying curve, with three drying ranges: constant drying to the critical moisture content (CMC), estimated around 65% herein; a marked decrease in drying to the fiber saturation point (FSP); and highly attenuated drying after this.

The moisture distributions had a marked parabolic shape, and the highly pronounced paraboloids at the beginning of the drying process diminished heavily to-

wards the end. These moisture distributions also showed marked asymmetry, indicating that the emission of surface moisture by convection was non-uniform. This emission is function of interface wood/drying environment, fluid and fluid flow of wet air. The last two aspects are responsible for mentioned asymmetry, like reported by Davis and Moore (1982).

Given the previous observations, we postulate that the mass convective coefficient values differ according to the surface contour: those parallel to the direction of the main flow are linear in distribution and normal contours are parabolic (see Fig. 3). Since all the moisture distributions were parabolic, we represented all the studied moisture ranges with only one EDC function, which is given by Eq. (2). Table 1 shows the parameters α, β and S, as determined for the studied transversal direction. The values reported for S are similar to those published Siau (1984) and Pang (1996). Likewise, the values of D for M around the FSP, shown in Figure 6, are comparable to those published by Davis *et al.* (2002) and Gatica *et al*. (2011) for radiata pine and Rozas *et al.* (2009) for slash pine (*Pinus elliottii*).

Table 1. EDC parameters α, β, and S.

D		$S*10^6$ (m^2/s)			
A	β	S_w	S_e	S_s	S_n
-21.05	18.50-	0.326	0.186	0.836	3.77

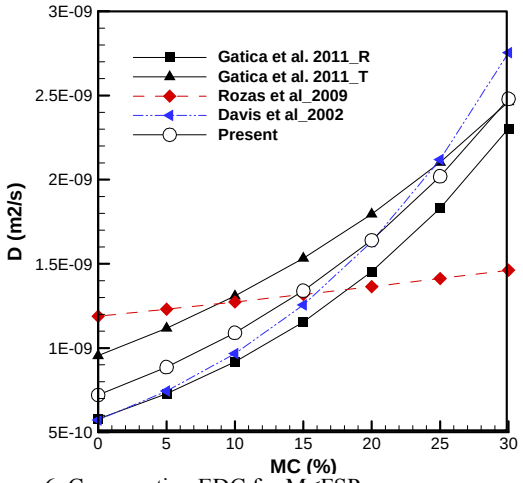

Figure 6. Comparative EDC for M<FSP.

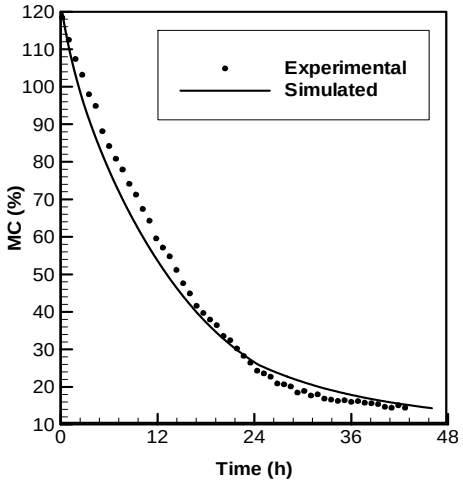

Figure 7. Drying curves.

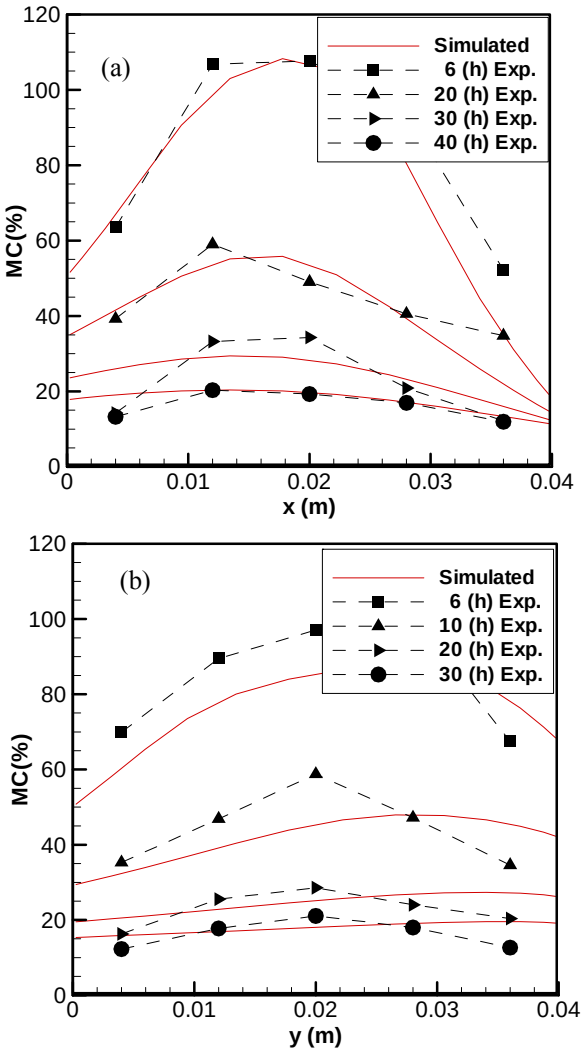

Figure 8. Average moisture distributions: a) along the x-axis, b) along the y-axis.

Figure 7 shows the experimental and numerical results of the drying curves, revealing that the simulated drying curve approaches the orderly dispersion of the experimental data obtained while continuously monitoring the weight of block P5 (differences below 5%).

Figures 8 show the average experimental and simulated spatial moisture distributions along the x and y directions after 6, 20, 30, and 40 h of drying. The distribution of the experimental data, which usually appear as parabolic distributions in simulations, were somewhat disorganized. The average differences were minimal (less than 0.1%) due to the search algorithm of the EDC function, which minimized said differences. However, maximum local differences reached around 10%.

Figure 9 is a three-dimensional representation of the discreet experimental values of the experimental moisture content for the different characteristic drying times (6, 20, 30, and 40 h) as opposed to a continuous representation of simulated values. This figure shows a highly variable distribution of the moisture content in time and space.

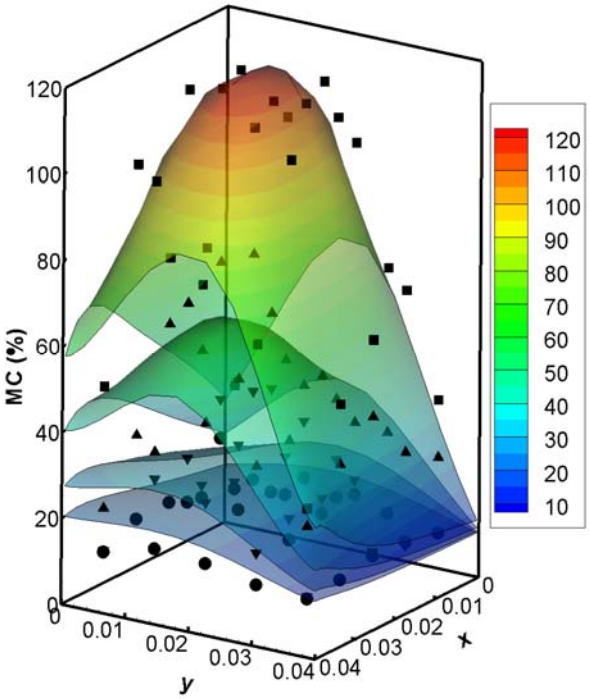

Figure 9. Experimental (discreet) and simulated (surface) moisture distributions for t= 6, 20, 30, and 40 (h).

Finally, Fig. 10 shows in detail the transitory non-uniform behavior of moisture distributions through moisture content isolines. We can observe: a) the transitory evolution of the maximum moisture content moving from the center towards the bottom right side (lower evaporation border), b) the accelerated drying of the upper and lower attack borders, and c) the marked asymmetry in drying between the upper and lower surface: attack and evaporation borders, respectively.

The latter justifies the non-uniform determination of S, differentiated according to contour orientation and position as diagrammed in Fig. 3.

V. CONCLUSIONS

The model presented herein allows us to simulate conventional, isothermal, two-dimensional drying of radiata pine wood based on the EDC.

In qualitative terms, the model satisfactorily simulated transitory non-homogenous distributions of moisture content.

Average moisture content values presented minimal deviations from the experimental data due to the EDC search methodology, which minimized the difference between experimental and numerical data.

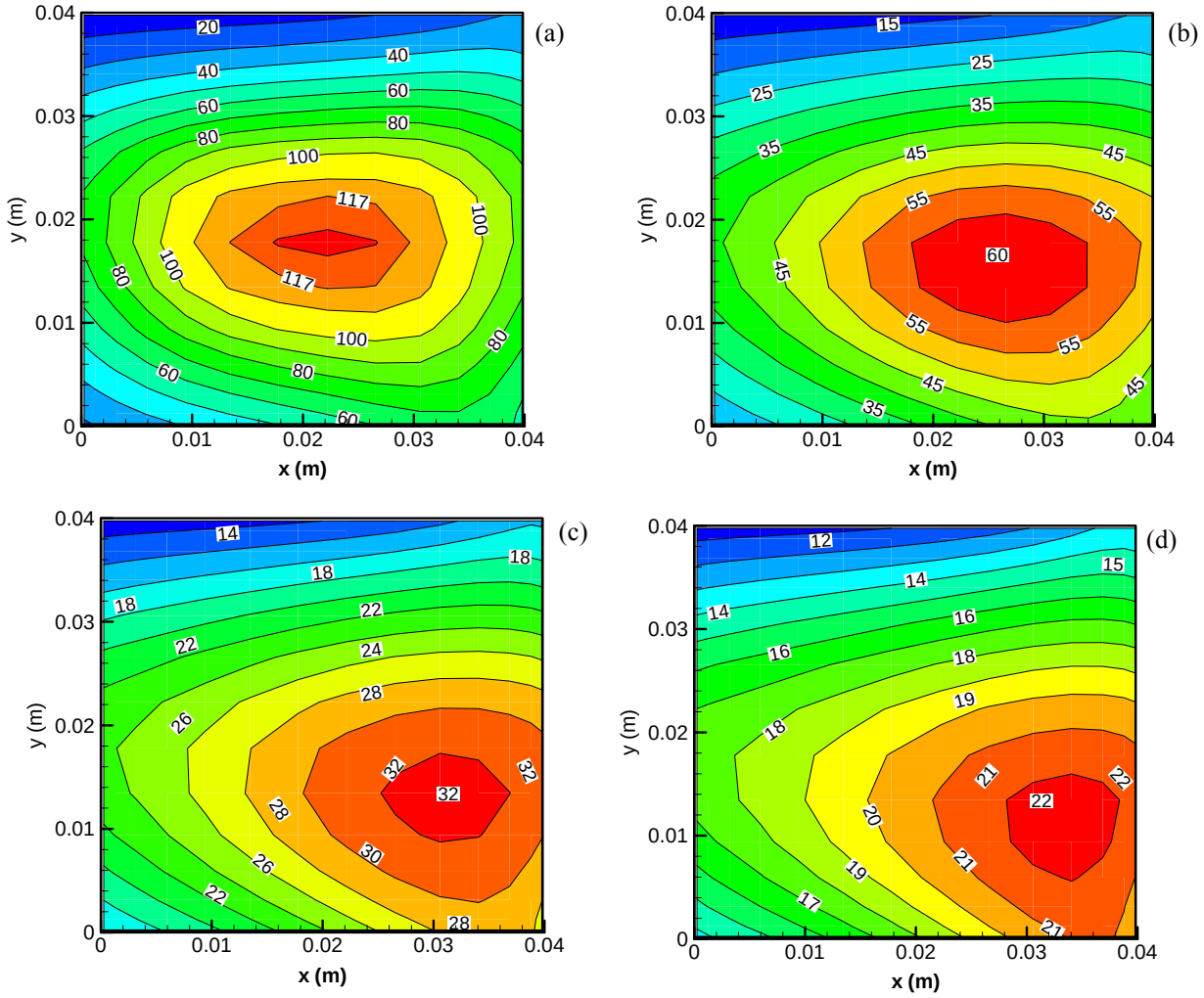

Figure 10. Isolines of moisture content: a) t=6 h, b) t=10 h, c) t=20 h, d) t=30 h.

The extensive search for the model parameters (α, β and S) resulted in highly effective simulations of the drying curve and the distribution of moisture content within the wood.

Considering variable and differentiated S values per contour type was a very effective strategy for modeling the high asymmetry of simulated two-dimensional drying.

Differentiating the EDC functions over and above the CMC, as done by Gatica *et al*. (2011), could significantly improve the proposed two-dimensional simulation, especially if the moisture range must be extended to include the green state.

NOMENCLATURE

P	Sample
E	Experiment
MC	Moisture Content (%)
M	Water mass (kg).
D	Effective diffusion coefficient (m2/s)
α, β	Effective Diffusion Constants
FSP	Fiber Saturation Point (M_m/M_d)
T	Temperature (K)
Error	Average error
t	Time (s)
x, y	Spatial co-ordinate (m)
L	Total length (m)
CMC	Critical Moisture Content (%)
S	**C**onvection coefficient (m/s)
a	Matrix coefficient
b	Vector coefficient
m	Mass (kg)
q	Mass flow (kg/m^2)
EDC	Effective Diffusion Coefficient
$\tilde{M}$	Mass ratio
g	Gravity (m/s^2)
n	Normal direction
Ω	Boundary
V	Domain
i, j	Knot
Δx, Δy	Mesh size

Subscripts

m	Moist
d	Dry
Sim	Simulated
Exp	Experimental
P	Finite volume center
W	Adjacent west finite volume center
E	Adjacent East finite volume center
N	Adjacent North finite volume center
S	Adjacent South finite volume center
w	Adjacent West boundary
e	Adjacent East boundary
n	Adjacent North boundary
s	Adjacent South boundary
i,j	knot
s	Surface
∞	Environment
0	Initial
min	Minimum
max	Maximum
opt	Optimum

REFERENCES

Bramhall, G. "Mathematical model for lumber drying. II. The model," *Wood Science*, **12**, 22-31 (1979).

Chen, X.D., "Moisture diffusivity in food and biological materials". *Drying Technology*, **25**, 1203-1213 (2007).

Cloutier, A. and Y. Fortín. "Moisture content- water potential relationship of wood from saturated to dry conditions," *Wood Science and Technology*, **25**, 263-280 (1991).

Cloutier, A. and Y. Fortin. "A model of moisture movement in wood based on water potential and the determination of the effective water conductivity," *Wood Science and Technology*. **27**, 95-114 (1993).

Comstock, G.L., "Moisture diffusion coefficients in wood as calculated from adsorption, desorption and steady state data," *Forest Products Journal*, **13**, 97–103 (1963).

Davis, R.W. and E.F. Moore, "A numerical study of vortex sheding from rectangles", *J. Fluid Mech.*, **116**, 475-506 (1982).

Davis, C.P., C.G. Carrington and Z.F. Sum, "The influence of compression wood on the drying curves of pinus radiata dried in dehumidifier conditions," *Drying Technology,* **20**, 2005-2026 (2002).

Droin A., J.L. Taverdet and J. M. Vergnaud, "Modeling the kinetics of moisture adsorption by wood," *Wood Sci Technol*. **22**, 11–20 (1988).

Gatica Y., C. Salinas, R. Ananías, "Modeling conventional one-dimensional drying of radiata pine based on the effective diffusion coefficient," *Latin American Applied Research*, **41**, 183-189 (2011).

Hukka, A., "The effective diffusion coefficient and mass transfer coefficient of nordic softwoods as calculated from direct drying experiments," *Holzforschung*, **53**, 534–540 (1999).

INN (Instituto Nacional de Normalización), *Madera. Determinación de humedad*. Chile, Santiago. NCh 176-1, of 84, parte 1 (1984).

INN (Instituto Nacional de Normalización), *Madera. Selección, obtención y acondicionamiento de muestras y probetas para la determinación de propiedades físicas y mecánicas.* Chile, Santiago. NCh 968. Of. 1986. (1986).

Jen, Y.L. and S. Cheng, "Solutions of Luikov equations of heat and mass transfer in capillary-porous bodies," *Int. J. Heat Mass Transfer,* **34**, 1747-1754 (1991).

Keey, R., T. Langrish and J. Walker, *Kiln DryingLlumber*. Spriger, N. York (2000).

Lapidus, L. and G.F. Pinder, *Numerical Solution of Partial Differential Equations in Science and Engineering*. John Wiley & Sons Inc. (1982).

Luikov, S.A., *Heat and Mass Transfer in Capillary Porous Bodies*. Pergamon Press, Oxford (1966).

Nabhani M., C. Tremblay and Y. Fortin, "Experimental determination of convective heat and mass transfer coefficients during wood drying," *8º International IUFRO wood drying conference*, 225-230 (2003).

Nasrallah, S.B. and P. Perré. "Detailed study of a model of heat and mass transfer during convective drying of porous media," *International journal of heat and mass transfer*, **31**, 957-967 (1988).

Pang, S., "Relationship between a diffusion model and a transport model for softwood drying," *Wood and Fiber Science*, **29**, 58-67 (1996).

Pang, S., "Moisture content gradient in a softwood board during drying: simulation from a 2D model and measurement," *Wood Science and Technology,* **30**, 165-178 (1997).

Patankar, S.V., *Numerical Heat Transfer and Fluid Flow*, Hemisphere Publishing Corporation, Washington, DC (1980).

Perré, P., M. Moser and M. Martin, "Advances in transport phenomena during convective drying with superheated steam and moist air," *International journal of heat and mass transfer*, **36**, 2725-2746 (1993).

Perré, P. and I. Turner, "A 3-D version of transpore: a comprehensive heat and mass transfer computational model for simulating the drying of porous media," *International Journal of heat and mass transfer,* **42**: 4501-4521 (1999).

Plumb, O.A., G.A. Spolek and B.A. Olmstead, "Heat and mass transfer in wood during drying," *Intern. J. Heat Mass Transfer,* **28**, 1669-1678 (1985).

Rozas, C., I. Tomaselli and E. Zanoelo, "Internal mass transfer coefficient during drying of softwood (Pinus elliotti) boards," *Wood Science and Technology,* **43**, 361-373 (2009).

Siau, J.F., *Transport Processes in Wood,* Springer, New York (1984).

Siau, J.F., *Wood: Influence of Moisture on Physical Properties*, VPI and State University, USA (1995).

Simpson, W.T., and J.Y. Liu, "An optimization technique to determine red oak surface and internal moisture transfer coefficients during drying," *Wood and Fiber Science,* **29**, 312–318 (1997).

Smith, S., and T. Langrish. "Multicomponent solid modeling of continuos and intermittent drying of Pinus radiata sapwood below the fiber saturation point," *Drying Technology*, **26**, 844-854 (2008).

Stamm, A., *Wood and Cellullose Science, Ch. 23: Diffusion in Wood*. Ronald Press, N. York (1964).

Tremblay, C., A. Cloutier and Y. Fortin, "Experimental determination of the convective heat and mass transfer coefficients for wood drying,". *Wood. Science and Technology*, **34,** 253-276 (2000).

Turner, I., "A two-dimensional orthotropic model for simulating wood drying processes," *Appl. Math. Modelling*. **20**, 60-81 (1996).

Whitaker, S., "Simultaneous heat, mass, and momentum transfer in porous media: A theory of drying," *Advances in Heat Transfer*, **13**, 119- 203 (1977).

Yang, R.J. and L.M. Fu, "Thermal and flow analysis of a heated electronic component," *Int. J. Heat and Mass Transfer,* **44**, 2261-2275 (2001).

Younsi, R., D. Kocaefe, S. Poncsak and Y. Kocaefe**. "**A Diffusion-based Model for Transient High Temperature Treatment of Wood," *Journal of building physics*, **30,** 113-135 (2006).

Received: May 11, 2011
Accepted: February 3, 2012
Recommended by subject editor: Adrian Lew